COHERENT VORTEX SIMULATION (CVS) OF A FLOW PAST A NACA AIRFOIL 23012 AT RE = 1000

Kai Schneider[1,2*] **and Marie Farge**[3†]

[1] Laboratoire de Modélisation et Simulation Numérique en Mécanique du CNRS
IMT - Technopôle de Château-Gombert
38 rue F. Joliot-Curie, 13541 Marseille Cedex 20, France

[2] Centre de Mathématiques et d'Informatique, Université de Provence
39 rue F. Joliot-Curie, 13543 Marseille Cedex 13, Marseille, France

[3] Laboratoire de Météorologie Dynamique du CNRS, Ecole Normale Supérieure
24 rue Lhomond, 75231 Paris Cedex 05, France

ABSTRACT

We present coherent vortex simulations of two–dimensional flows past the NACA 23012 airfoil at Reynolds number 1000. The incompressible Navier–Stokes equations in vorticity–velocity formulation are discretized first in time using a second order semi–implicit scheme. The spatial discretization is based on an adaptive wavelet method with automatic grid refinement. In this Petrov–Galerkin scheme the vorticity field is developed into an orthogonal wavelet series and the test functions are chosen as solutions of the linear part of the equation. The shape of the airfoil together with no–slip boundary conditions are imposed using a volume penalisation method. The presented results show the ability of the CVS method to deal with complex geometies.

INTRODUCTION

Recently, we proposed a new CFD method, called Coherent Vortex Simulation (CVS) [5, 6], for computing fully developed turbulent flows. It results from the observation that turbulent flows contain both an organized part (the coherent vortices) and a random part (the incoherent background flow) [5, 7]. The CVS method is based on the wavelet filtered Navier-Stokes equations, which corresponds to the coherent flow whose evolution is computed deterministically in an adaptive wavelet basis [8], [11]. The influence of the incoherent background flow onto the coherent flow is either statistically modelled or simply neglected. For applications to compute three–dimensional turbulent mixing layers we refer to [13].

In this paper we present applications of the CVS method to compute two–dimensional flows past NACA airfoils. We use an adaptive wavelet method with automatic grid refinement to integrate the velocity-vorticity formulation of the two-dimensional Navier-Stokes equations [8, 10]. To take into account complex geometries, we propose to couple the CVS method we have developed with the penalisation technique, introduced by Arquis and Caltagirone [3]. Therewith walls or solid obstacles, even if their shape varies in time, are modelled as a porous medium whose porosity η tends to zero. A mathematical theory proving convergence of this physically based approach has been given by Angot et al. [2]. This technique has been applied in the context of low order methods (finite difference/volume schemes, e.g. [2]) and also with spectral methods e.g. [9, 12]. The motivation to couple the penalisation technique with an adaptive wavelet solver comes from the fact that adaptive wavelet methods dynamically refine the grid in regions of strong gradients. Hence, we expect the solver to adapt automatically, not only to the evolution of the flow, but also to the geometry of walls or bluff bodies.

The paper is organised as follows: first we present the penalisation method together with the discretization used to solve the penalised Navier-Stokes equations numerically. As application we present numerical simulations of 2D viscous incompressible flow around a NACA airfoil, which is impulsively started. Finally, we give some conclusions and perspectives for turbulence modeling of bluff body flows.

THE PENALISATION METHOD AND THE NUMERICAL DISCRETISATION

Governing equations

The penalisation technique is based on the physical idea which consists in modeling solid walls or obstacles as porous media whose porosity η is tending to zero [3]. The geometry is described by a mask function $\chi(\vec{x})$ which is 1 inside the solid regions and 0 elsewhere. Note that the penalisation method can also take into account obstacles with time–varying shape by simply introducing a time–dependent mask function. The Navier-Stokes equations are modified by adding a supplementary term containing the mask function. For the penalised velocity $\vec{u}_\eta$ we obtain

$$\partial_t \vec{u}_\eta + \vec{u}_\eta \cdot \nabla \vec{u}_\eta + \nabla p_\eta - \nu \nabla^2 \vec{u}_\eta + \frac{1}{\eta} \chi_{\Omega_s} (\vec{u}_\eta - \vec{u}_p(t)) = 0 \quad (1)$$

where $\vec{u}_\eta(\vec{x}, t)$ is the flow velocity, $p_\eta(\vec{x}, t)$ the pressure, $\vec{u}_p(t)$ the obstacle's velocity (assumed to be zero here), and ν the kinematic viscosity. In the following the density ρ is normalized to 1. The mask function to take into account the

*kschneid@cmi.univ-mrs.fr
†farge@lmd.ens.fr

geometry of the airfoil is given by

$$\chi_{\Omega_s}(\vec{x}) \;=\; \begin{cases} 1 & \text{for} \quad \vec{x} \in \bar{\Omega}_s \\ 0 & \text{elsewhere} \end{cases} \tag{2}$$

where Ω_s denotes the volume of the airfoil. For $\eta \longrightarrow 0$ the flow evolution is governed by the Navier–Stokes equations in the fluid regions, and by Darcy's law, i.e. the velocity is proportional to the pressure gradient, in the solid regions where obstacles or walls are present. In [2] a mathematical proof has been given that the above equations converge towards the Navier–Stokes equations with no-slip boundary conditions, with order $\eta^{3/4}$ inside the obstacle and with order $\eta^{1/4}$ elsewhere, in the limit η tending to zero. In numerical simulations an improved convergence of order η has been reported [2], [9].

The resulting forces $\vec{F}$ on the obstacle, i.e. drag and lift ,can be computed by integrating the penalised velocity over the obstacle's volume [2]:

$$\vec{F} \;=\; \lim_{\eta \to 0} \int_{\Omega_s} \nabla p_\eta \, dx \;=\; -\lim_{\eta \to 0} \frac{1}{\eta} \int_{\Omega_s} \vec{u}_\eta \, dx \tag{3}$$

$$= \int_{\partial\Omega_s} \sigma(\vec{u}, p) \cdot \vec{n}_f \, d\gamma \tag{4}$$

where Ω_s is the obstacle's volume, $\partial\Omega_s$ its boundary, $\vec{n}$ its outer normal and $\sigma(\vec{u}, p) \;=\; \frac{1}{2\nu}\,(\nabla\vec{u} + (\nabla\vec{u})^t) - pI$ the stress tensor. Hence, the lift and drag forces on the obstacle, i.e. forces parallel and perpendicular to the free–stream velocity of the flow, are easy to compute as volume integrals instead of contour integrals.

For two–dimensional flows the vorticity–velocity formulation is prefered and therefore we take the curl of eq. (1), and we get

$$\begin{aligned} &\partial_t \omega_\eta \;+\; (\vec{u}_\eta + \vec{U}_\infty) \cdot \nabla\omega_\eta - \nu\,\nabla^2\,\omega_\eta \\ &\quad + \nabla \times \Big(\frac{1}{\eta}\,\chi_{\Omega_s}\,(\vec{u}_\eta) - \vec{u}_p(t)\Big) \;=\; 0 \end{aligned} \tag{5}$$

where $\omega = \nabla \times \vec{u}$ is the vorticity and $\vec{U}_\infty$ is the free–stream velocity, defined as $\lim_{|\vec{x}| \longrightarrow \infty} \vec{u}(\vec{x}) = \vec{U}_\infty$.

Adaptive wavelet discretization

For the numerical solution of the penalised equations we employ a wavelet scheme with adaptive grid refinment [8, 10, 11]. As adaptive schemes dynamically adapt the spatial grid at each time step, we first discretize the equations (6) in time using semi-implicit finite differences, i.e. Euler–backwards for the viscous term and Adams–Bashforth extra-polation for the nonlinear term, which are both of second order.

The resulting elliptic problem to be solved at each time step is:

$$\begin{aligned} (\gamma I - \nu\nabla^2)\omega^{n+1} = \frac{4}{3}\gamma\omega^n - \frac{1}{3}\gamma\omega^{n-1} - \nabla\cdot(\omega^\star\,\vec{u}^\star) \\ -\nabla\times\Big(\frac{1}{\eta}\,\chi\,(\vec{u}^\star - \vec{u}_p)\Big) \end{aligned} \tag{6}$$

where

$$\omega^\star = 2\,\omega^n - \omega^{n-1} \qquad \vec{u}^\star = 2\,\vec{u}^n - \vec{u}^{n-1} \tag{7}$$

with time step Δt, $\gamma = 3/(2\Delta t)$ and I representing the identity.

For the space discretization we use a Petrov–Galerkin scheme. Therefore the vorticity is developed into a set of trial functions and the minimization of the weighted residual of (6) requires that the projection onto a space of test functions vanishes. As space of trial functions we employ a two-dimensional multiresolution analysis (MRA) [4] and develop ω^n at time step n into an orthonormal wavelet series

$$\omega^n(x,y) \;=\; \sum_\lambda \langle \omega^n \,,\, \psi_\lambda \rangle \; \psi_\lambda(x,y) \tag{8}$$

with the multi–index $\lambda = (j, i_x, i_y, \mu)$, where $j = 0, J_{max} - 1$ denotes the scale 2^{-j+1}, $(i_x, i_y) = 0, ..., 2^j - 1$ the position and $\mu = 1, 2, 3$ the three different directions of the wavelets.

The test functions θ_λ are defined as solutions of the linear part of eq. (6)

$$(\gamma I - \nu\nabla^2)\theta_\lambda \;=\; \psi_\lambda \tag{9}$$

and can be computed in a preprocessing step. This avoids assembling the stiffness matrix and solving a linear equation at each time step. The functions θ, called vaguelettes, are explicitely calculated in Fourier space and have similar localization properties as wavelets [8]. The solution of (6) in wavelet space therewith reduces to a change of basis:

$$\begin{aligned} \tilde{\omega}_\lambda \;&=\; \langle \omega^{n+1} \,,\, \psi_\lambda \rangle \\ &=\; \langle (\frac{4}{3}\gamma\omega^n - \frac{1}{3}\gamma\omega^{n-1} - \nabla\cdot(\omega^\star(\vec{u}^\star)) \\ &-\; \nabla\times(\frac{1}{\eta}\chi(\vec{u}^\star - \vec{u}_p))), \theta_\lambda \rangle \quad . \end{aligned} \tag{10}$$

Nonlinear wavelet thresholding is applied in each time step to obtain an adaptive discretization by retaining only those wavelet coefficients $\tilde{\omega}_\lambda$ with absolute value above a given threshold $\epsilon = \epsilon_0\sqrt{Z}$, where ϵ_0 is a constant and $Z = \frac{1}{2}\int |\omega(\vec{x})|^2 d\vec{x}$ is the enstrophy. For the next time step the index coefficient set (which addresses each coefficient in wavelet space) is determined by adding neighbours to the retained wavelet coefficients. Consequently, only those coefficients $\tilde{\omega}$ in (10) belonging to this extrapolated index set are computed using the adaptive vaguelette decomposition [8]. The nonlinear term $-\nabla\cdot(\omega^\star(\vec{u}^\star)) - \nabla\times(\frac{1}{\eta}\,\chi\,(\vec{u}^\star - \vec{u}_p))$ is evaluated by partial collocation on a locally refined grid [11]. The vorticity $\omega^\star$ is reconstructed in physical space on an adaptive grid from its wavelet coefficients $\tilde{\omega}^\star$ using the adaptive wavelet reconstruction algorithm [8]. From the adaptive vaguelette decomposition with $\theta = (\nabla^2)^{-1}\,\psi$, we solve $\nabla^2\Psi^\star = \omega^\star$ to get the stream function $\tilde{\Psi}^\star$ and reconstruct $\Psi^\star$ on a locally refined grid. By means of centered finite differences of 4th order we compute $\nabla\omega^\star$, $\vec{u}^\star \;=\; (-\partial_y\Psi^\star, \partial_x\Psi^\star)$ and $\nabla\times(\frac{1}{\eta}\;\chi\,(\vec{u}^\star - \vec{u}_p))$ on the adaptive grid. Subsequently, the nonlinear term is summed up pointwise, and finally (10) is solved using the adaptive vaguelette decomposition.

NUMERICAL RESULTS FOR THE NACA 23012 AIRFOIL

The five-digit NACA series of airfoils were developed by Eastman N. Jacobs in 1935. The position of maximum camber is unusually far forward, within $5 - 15\%$ of the chord length from the leading edge. These airfoils had higher maximum lift coefficients and lower pitching moments than the NACA four-digit series. Following Jacobs the best airfoil in that series was the NACA 23012 airfoil [1]. The NACA 23012 airfoil section was used in the Douglas DC-4, a transporter with four engines during World War II [1].

Here we present CVS computations of a flow around the NACA 23012 airfoil at $Re = 1000$, which has been impulsively started with an angle of incidence of 30°. The flow

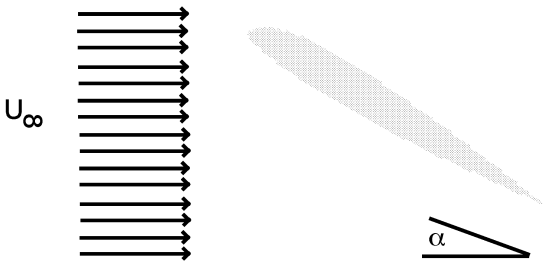

Figure 1: Flow configuration. Airfoil NACA 23012, $\alpha = 30°$.

configuration is depicted in Fig. 1. Fig. 2 shows the isolines of vorticity at 4 different time instants using CVS. We observe at early time the formation of a small vortex at the trailing edge which then detaches and is advected by the mean flow. In Fig. 3 we plot the time evolution of the enstrophy, which increases until the trailing vortex detaches and then continuously decreases. In the future we shall present several results (lift and drag coefficients) of CVS computations for different angles of attack together with comparisons with results obtained by DNS using a classical spectral method.

CONCLUSIONS AND PERSPECTIVES

In the paper we have presented an adaptive wavelet method, called Coherent Vortex Simulation (CVS), coupled with a volume penalisation technique, to compute two–dimensional turbulent flows in complex geometries. This numerical scheme allows automatic adaption of the grid, not only to the evolution of the flow, but also to the geometry of walls or bluff bodies. We presented CVS of 2D incompressible viscous flows past a NACA 23012 airfoil at $Re = 1000$. In future work, we will also apply the CVS approach to compute 2D and 3D bluff body flows at higher Reynolds numbers [6].

Acknowledgements: We thankfully acknowledge financial support from the European Union project IHP on 'Breaking complexity'.

*

References

[1] J.D. Anderson. *A History of Aerodynamics.* Cambridge University Press, 2000.

[2] P. Angot, C.-H. Bruneau and P. Fabrie. A penalisation method to take into account obstacles in viscous flows. *Num. Math.*,**81**, 497–520, 1999.

[3] E. Arquis and J.P. Caltagirone. Sur les conditions hydrodynamiques au voisinage d'une interface milieu fluide – milieux poreux: application à la convection naturelle. *C. R. Acad. Sci. Paris II*, **299**, 1–4, 1984.

[4] M. Farge. Wavelet transforms and their applications to turbulence. *Ann. Rev. Fluid Mech.*, 24:395, 1992.

[5] M. Farge, K. Schneider and N. Kevlahan. Non–Gaussianity and Coherent Vortex Simulation for two–dimensional turbulence using an adaptive orthonormal wavelet basis. *Phys. Fluids*, **11**(8), 2187–2201, 1999.

[6] M. Farge and K. Schneider. Coherent Vortex Simulation (CVS), a semi–deterministic turbulence model using wavelets, *Flow, Turbulence and Combustion*, **66**(4), 393–426, 2001

[7] M. Farge, K. Schneider, G. Pellegrino, A. Wray and B. Rogallo. Coherent vortex extraction in three–dimensional homogeneous turbulence: comparison between CVS–wavelet and POD–Fourier decompositions, *Phys. Fluids*, **15**(10), 2886–2896, 2003.

[8] J. Fröhlich and K. Schneider. An adaptive wavelet–vaguelette algorithm for the solution of PDEs, *J. Comput. Phys.*, **130**, 174–190, 1997.

[9] N. Kevlahan and J.-M. Ghidaglia. Computation of turbulent flow past an array of cylinders using a spectral method with Brinkman penalization. *Eur. J. Mech./B*, **20**, 333–350, 2001.

[10] K. Schneider, N. Kevlahan and M. Farge. Comparison of an adaptive wavelet method and nonlinearly filtered pseudo-spectral methods for two-dimensional turbulence. *Theoret. Comput. Fluid Dynamics*, **9** (3/4), 191–206, 1997.

[11] K. Schneider and M. Farge. Adaptive wavelet simulation of a flow around an impulsively started cylinder using penalisation. *Appl. Comput. Harm. Anal.*, **12**, 374–380, 2002.

[12] K. Schneider. Numerical simulation of the transient flow behaviour in chemical reactors using a penalisation method. *Computers & Fluids*, 2005, in press.

[13] K. Schneider, M. Farge, G. Pellegrino & M. M. Rogers CVS filtering of 3D turbulent mixing layers using orthogonal wavelets. *J. Fluid Mech.*, May 2005, in press.

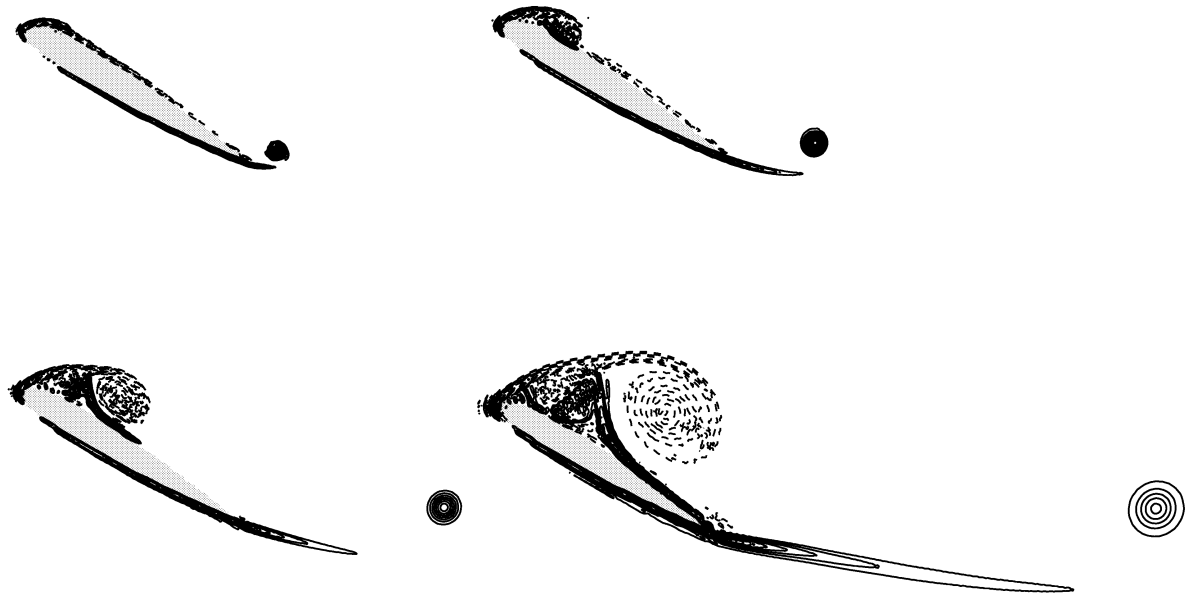

Figure 2: Airfoil NACA 23012, $\alpha = 30°$, $Re = 1000$. Isolines of vorticity at instances $T = 0.2, 0.5, 1.0, 2.0$.

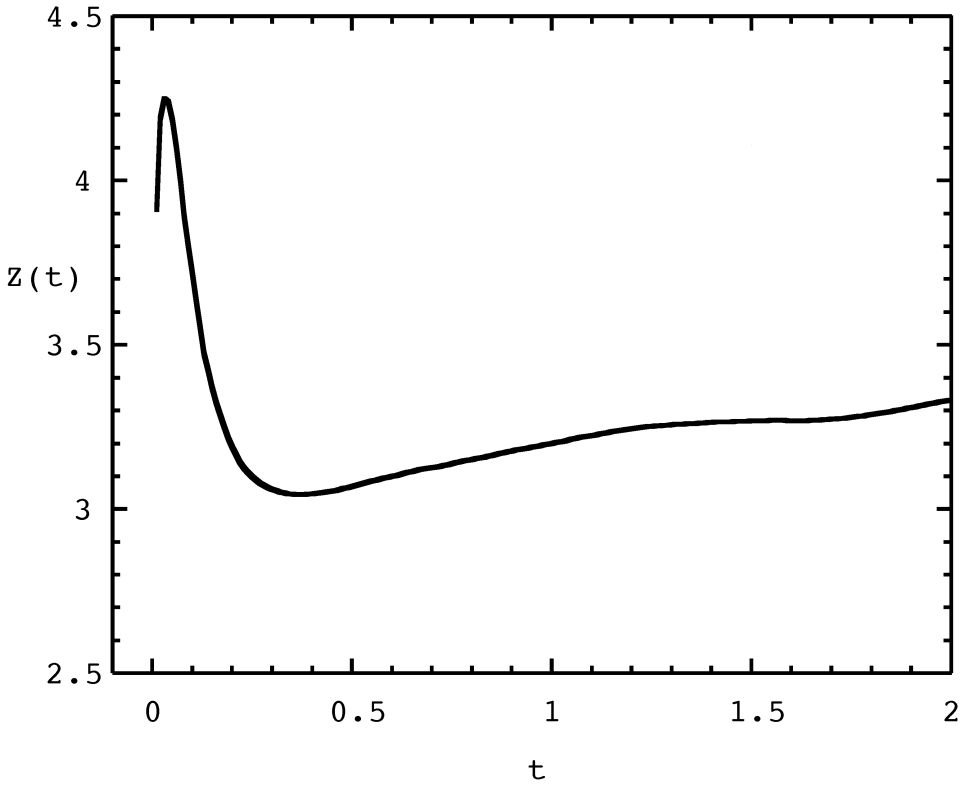

Figure 3: Airfoil NACA 23012, $\alpha = 30°$, $Re = 1000$. Time evolution of total enstrophy.